Coordinated Phase-Based Voltage Regulation in Active Unbalanced LV Distribution Networks

Georgios C. Kryonidis, Eleftherios O. Kontis, Andreas I. Chrysochos,
Charis S. Demoulias, and Grigoris K. Papagiannis*
School of Electrical and Computer Engineering, Aristotle University of Thessaloniki, Thessaloniki, Greece
*corresponding author's e-mail: grigoris@eng.auth.gr

***Abstract*—In this paper, a phase-based control algorithm is proposed to effectively address the voltage regulation problem in unbalanced low-voltage (LV) networks with high photovoltaic (PV) penetration. The proposed method is based on a single-phase droop characteristic of the injected power with respect to the phase-to-neutral voltage at the point of common coupling for each PV unit. The main objective is to regulate efficiently the grid phase voltages, as well as to ensure a uniform active power curtailment among the PV units connected in the same phase. Simulations of a highly unbalanced LV network justify the validity of the proposed method and its enhanced performance over the conventional droop control in terms of overvoltage and unbalance mitigation.**

***Index Terms*—Active power curtailment, distributed generation, sensitivity theory, unbalanced distribution network, voltage regulation.**

I. Introduction

Nowadays, distribution system operators (DSOs) face a series of technical challenges, raised by the proliferation of distributed generation and especially of photovoltaic (PV) units [1]. Voltage rise is considered as the major obstacle, limiting the further penetration of distributed generation [2]. This occurs mostly in low-voltage (LV) networks, since their resistive nature introduces a strong coupling between the active power and grid voltage [3]. Moreover, the voltage rise problem can be further deteriorated by the inherent network asymmetries, which are caused by the single-phase loads and the arbitrary connection of small single-phase PV units in the different grid phases [4].

The available solutions to tackle overvoltages in distribution grids include grid reinforcement, reactive power control, active power curtailment (APC) techniques, and the on-load tap changer (OLTC) control of the medium-/low-voltage (MV/LV) transformer [5]-[10]. Among them, grid reinforcement is not a preferable option for the DSOs, due to the high investment costs [5]. The OLTC control option is also an expensive solution, since it requires the replacement of the existing MV/LV transformers with new ones equipped with OLTC [6]. The participation of PV units in the voltage regulation process by means of reactive power control has been already incorporated into several national grid codes [7], [8]. However, reactive power control is rather ineffective in LV networks, due to their resistive behavior and the limited reactive power capability of the grid-interfaced inverters [9],[10].

The voltage rise problem in LV distribution networks can be effectively addressed by incorporating APC techniques into the PV units [11], [12]. The $P(V)$ droop characteristic is the most widely-known decentralized voltage regulation method, where the injected power is partially curtailed based only on local voltage measurements [13]. Nevertheless, the amount of curtailed power and overall energy in each PV unit is very sensitive to the voltage magnitude at the point of common coupling (PCC). The PCC voltage is mainly affected by two factors: The relative location of the PV unit with respect to the MV/LV transformer and the connection phase. As a result, overvoltages are more likely to occur at the lightly loaded phases of the most distant network nodes, with the corresponding PV units curtailing more active power compared to the other PV units in the same phase or feeder [14].

In the literature, a coordinated procedure has been already proposed to overcome this problem [14], [15]. Specifically, the droop characteristics are recalculated on a regular basis to alleviate the PV units located at the distant nodes from the excessive active power curtailment. This is achieved by a uniform reallocation of the amount of curtailed power among all the PV units of the network. This method is straightforward, allowing the implementation of different power curtailing policies among the PV units. However, the main drawback is its applicability in heavily unbalanced LV networks, since the analysis assumes balanced network operation, which is a rather unrealistic case if single PV units are used.

In this paper, a phase-based, coordinated active power curtailment (CAPC) method is introduced to achieve uniform active power curtailment among PV units connected at the same phase of the network. This method is implemented by using the asymmetrical sensitivity matrix of the network, to properly recalculate the single-phase droop characteristics in each single-phase and/or three-phase PV unit. In this way, the voltage asymmetries can be reduced, while the overall voltage profile is improved and thus the overall PV penetration can be further increased.

This work is supported by the European FP7 program, under the project: FP7 INCREASE, http://www.project-increase.eu/.

The work of G. C. Kryonidis is supported by the Research Committee of Aristotle University of Thessaloniki via a merit scholarship between 2016 and 2017.

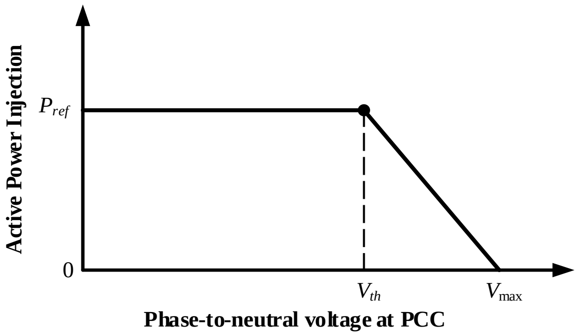

Fig. 1. Single-phase droop control.

II. Proposed Method

The proposed voltage regulation method exploits the sensitivity matrix of the asymmetrical network to coordinate the single-phase droop characteristics of the PV units. In the next subsections, the theoretical background of the droop control and the implementation of the proposed CAPC method are presented.

A. Droop Control

The main objective of the droop control is to prevent PV units from overvoltage tripping that may occur during high generation periods [13]. This is attained by curtailing part of the active power injection of the PV units in order to mitigate overvoltages. In this paper, a single-phase approach of the droop control is adopted, in which the active power injection is determined for each phase with respect to the corresponding phase-to-neutral PCC voltage. This is implemented by the droop curve of Fig. 1, consisting of three operational regions. In the first region, the active power is equal to a predefined value (P_{ref}), provided that the PCC voltage remains below the voltage threshold (V_{th}). Generally, this value is equal to the maximum power point (MPP) that the PV unit can deliver at a specific time instant. However, in case the CAPC method is activated, new settings concerning this value may be defined. In the second region, the APC is activated, while in the third one, the injected power is zeroed when the PCC voltage exceeds the maximum voltage threshold ($V_{\max}$). In this paper, $V_{\max}$ is set equal to the maximum permissible voltage limit of 1.1 p.u., according to the EN50160 Standard [16], in order to ensure effective overvoltage mitigation.

Another implementation of active power droop control assumes that the active power injection in each phase is calculated with respect to the positive-sequence component of the PCC voltage [15]. The drawback of this approach is that it neglects the network asymmetries and therefore cannot ensure overvoltage and/or voltage unbalance mitigation. On the other hand, in the single-phase droop control, network voltages are individually controlled in each phase, thus enhancing the performance of the control compared to the positive-sequence approach.

B. Coordinated Active Power Curtailment

Scope of the proposed method is to achieve a uniform active power curtailment among the PV units connected in the same phase. To implement this, the utilization of the sensitivity matrix of the asymmetrical network is required. Generally, as shown in (1), the sensitivity matrix is used as a measure to quantify the impact of active and reactive power variations in each phase, with respect to the phase-to-neutral network voltage magnitude and angle.

$$\begin{bmatrix} \Delta\boldsymbol{\theta}_a \\ \vdots \\ \Delta\boldsymbol{V}_c \end{bmatrix} = \begin{bmatrix} \boldsymbol{S}_{P_a}^{\theta_a} & \cdots & \boldsymbol{S}_{Q_c}^{\theta_a} \\ \vdots & \ddots & \vdots \\ \boldsymbol{S}_{P_a}^{V_c} & \cdots & \boldsymbol{S}_{Q_c}^{V_c} \end{bmatrix} \begin{bmatrix} \Delta\boldsymbol{P}_a \\ \vdots \\ \Delta\boldsymbol{Q}_c \end{bmatrix} \tag{1}$$

$\Delta\boldsymbol{\theta}_x$ and $\Delta\boldsymbol{V}_x$ are the voltage angle and magnitude variation vectors in each phase, respectively, with their dimensions being equal to the number of network nodes (n). Subscript x indicates one of the three network phases. $\Delta\boldsymbol{P}_x$ and $\Delta\boldsymbol{Q}_x$ are the vectors of active and reactive power variation in each phase, while $\boldsymbol{S}_{P_x}^{\theta_x}$, $\boldsymbol{S}_{Q_x}^{\theta_x}$, $\boldsymbol{S}_{P_x}^{V_x}$, and $\boldsymbol{S}_{Q_x}^{V_x}$ are the corresponding n-th order square submatrices of the asymmetrical sensitivity matrix.

In this paper, the sensitivity matrix of (1) is obtained by employing the perturb-and-observe algorithm. According to this, the active and reactive power at each node and phase of the network are deliberately perturbed. By performing power flow calculations, the corresponding phase-to-neutral voltage variations at each network node are calculated. Therefore, the ratio of voltage magnitude and angle variations with respect to active and reactive power variations forms the elements of the asymmetrical sensitivity matrix.

The incorporation of the single-phase droop control into the PV units results in the overvoltage mitigation. Nevertheless, the uncoordinated implementation of the $P(V)$ droop characteristics invokes a non-uniform distribution of the curtailed power among the PV units. The proposed method aims to address this issue by redistributing the active power curtailment among the PV units, while maintaining an almost similar voltage profile in each phase. For this purpose, the following equation is employed:

$$V_{set,x} = V_{mpp,i\,(x)} - V_{droop,i\,(x)} \tag{2}$$

where $V_{droop,i\,(x)}$ and $V_{mpp,i\,(x)}$ are the phase-to-neutral voltage magnitudes of the i-th node provided the droop control is activated and the PV units inject their MPP, respectively. $i(x)$ refers to the node with the maximum phase-to-neutral voltage after the activation of the single-phase droop control, while $V_{set,x}$ is the corresponding voltage difference. Eq. (2) is employed to achieve similar voltage profiles between the APC and CAPC methods.

Furthermore, in order to redistribute the overall curtailed power among the PV units with respect to the corresponding MPP at each time instant, the coefficient vector ($\boldsymbol{w}_x$) is introduced and is calculated for each phase according to

$$\boldsymbol{w}_x = \frac{\boldsymbol{P}_{mpp,x}}{\min(\boldsymbol{P}_{mpp,x})} \tag{3}$$

where $\boldsymbol{P}_{mpp,x}$ is the per phase vector of dimension n containing the MPP of each network node. In case of network nodes with no PV injection, the corresponding elements of the coefficient vector are set to zero. To calculate the active power curtailment in each phase, the following system of equations must be solved:

$$\begin{bmatrix} V_{set,a} \\ V_{set,b} \\ V_{set,c} \end{bmatrix} = \begin{bmatrix} \boldsymbol{w}_a \boldsymbol{S}_{P_a}^{V_{i(a)}} & \boldsymbol{w}_b \boldsymbol{S}_{P_b}^{V_{i(a)}} & \boldsymbol{w}_c \boldsymbol{S}_{P_c}^{V_{i(a)}} \\ \boldsymbol{w}_a \boldsymbol{S}_{P_a}^{V_{i(b)}} & \boldsymbol{w}_b \boldsymbol{S}_{P_b}^{V_{i(b)}} & \boldsymbol{w}_c \boldsymbol{S}_{P_c}^{V_{i(b)}} \\ \boldsymbol{w}_a \boldsymbol{S}_{P_a}^{V_{i(c)}} & \boldsymbol{w}_b \boldsymbol{S}_{P_b}^{V_{i(c)}} & \boldsymbol{w}_c \boldsymbol{S}_{P_c}^{V_{i(c)}} \end{bmatrix} \begin{bmatrix} P_{curt,a} \\ P_{curt,b} \\ P_{curt,c} \end{bmatrix} \tag{4}$$

Here $P_{curt,x}$ is a scalar, representing the amount of active power which will be curtailed from the PV unit with the minimum MPP power in each phase. The new injection set-points for all PV units are calculated as follows:

$$\boldsymbol{P}_{inj,x} = \boldsymbol{P}_{mpp,x} - \boldsymbol{w}_x P_{curt,x} \tag{5}$$

where $\boldsymbol{P}_{inj,x}$ is the per phase vector of the injected active power of the PV units.

The single-phase droop characteristics are recalculated according to the new power injections. For this purpose, a power flow calculation is conducted with the new set-points to acquire the new network voltages. Thus, a unique pair of phase-to-neutral voltage (V_{new}) and single-phase active power injection (P_{inj}) is created for each PV unit. Based on which operation region of the droop characteristic the above pair belongs to, two cases are considered:

- $V_{new} < V_{th}$ – In this case, the PV unit operates in the first region of Fig. 1. Therefore, P_{ref}^{new} is set equal to P_{inj} and the voltage thresholds V_{th} and $V_{\max}$ remain unchanged.
- $V_{new} > V_{th}$ – In this situation, the PV unit operates in the second region where the APC method is activated. $V_{\max}$ is kept constant to 1.1 p.u., while the remaining settings of the droop characteristic, i.e. P_{ref}^{new} and V_{th}^{new}, are recalculated. Priority is given on maintaining constant V_{th}. Therefore, the P_{ref}^{new} is calculated as follows:

$$P_{ref}^{new} = P_{inj} \frac{V_{th} - V_{\max}}{V_{new} - V_{\max}} \tag{6}$$

Nevertheless, in case the calculated P_{ref}^{new} exceeds the MPP that the PV unit can deliver at the specific time instant, then P_{ref}^{new} is set equal to P_{mpp} and V_{th}^{new} is calculated according to

$$V_{th}^{new} = V_{\max} + \frac{P_{ref}^{new}}{P_{inj}} (V_{new} - V_{\max}) . \tag{7}$$

C. Implementation of the CAPC Method

An hierarchical control structure is adopted to implement the proposed CAPC method. For this purpose, a central controller monitors the network and determines the set-points for all PV units at each time instant. This controller is often located at the DSO level. The actual implementation of the CAPC method is depicted in Fig. 2 by means of a flowchart and consists of 7 Steps, described in detail below:

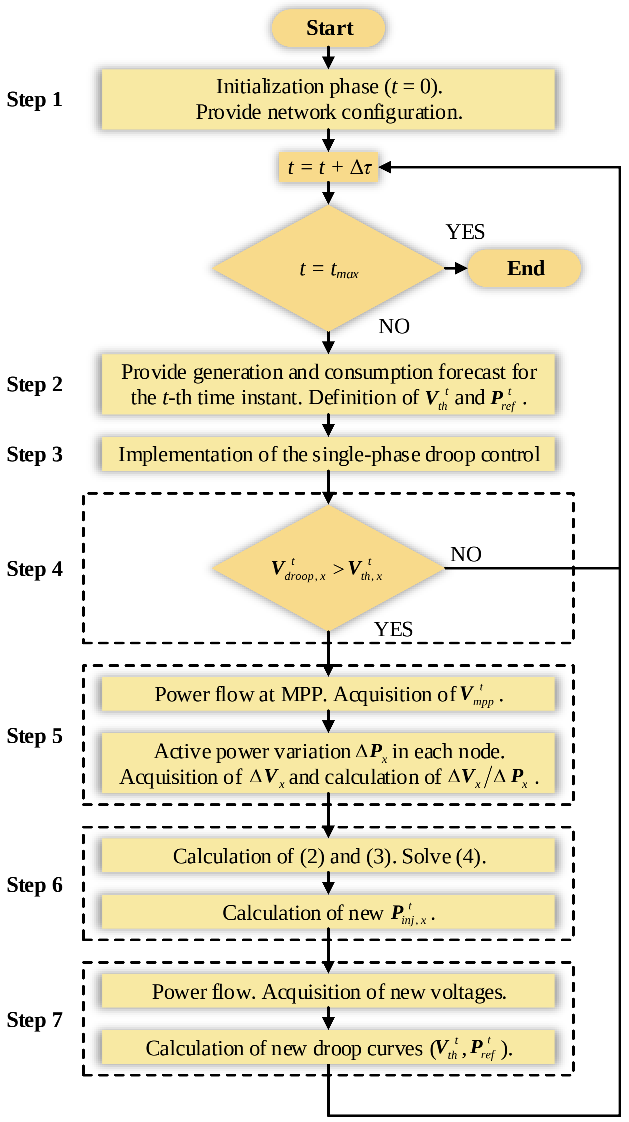

Fig. 2. Actual implementation of the proposed method.

Step 1: *Initialization phase*. The data related to the network configuration are forwarded to the central controller.

Step 2: *Consumption and generation forecast acquisition*. At each time instant (t), the central controller is updated with generation and consumption forecasts of the next time interval ($\Delta\tau$) and determines the initial settings of the droop characteristic in each PV unit as follows:

- P_{ref} is equal to the MPP of the corresponding PV unit.
- V_{th} and $V_{\max}$ are equal to 1.06 p.u. and 1.1 p.u., respectively. These values are fully configurable and can be defined by the DSO.

Step 3: *Implementation of the APC method*. The single-phase droop control is activated and a simulation is performed based on the forecasted values.

Step 4: *Check for the activation of the CAPC method*. Results obtained from the simulation of the previous Step are evaluated to check whether the CAPC method will be activated. In case active power curtailment occurs, the CAPC method is activated. Otherwise, the settings of all PV units remain unchanged and the procedure moves to the next time instant ($t+\Delta\tau$).

Step 5: *Sensitivity matrix calculation*. A power flow analysis is performed to calculate the network voltages ($\boldsymbol{V}_{mpp}^{t}$), when all PV units operate at their MPP. Furthermore, the active power at each network node and phase is deliberately perturbed to obtain the corresponding voltage variations and thus the asymmetrical sensitivity matrix. In this paper, only the sub-matrix referring to phase-to-neutral voltage magnitude variations with respect to the active power variations is required.

Step 6: *Calculation of new-injection set-points*. Using (2)-(5), the central controller calculates the new active power injection set-points. In this way, uniform active power curtailment among the PV units connected to the same phase is achieved.

Step 7: *Recalculation of the droop characteristics*. Based on the new injection set-points, a power flow is conducted to obtain the new network voltages. Then, the new droop curves are recalculated following the process described in the previous subsection and forwarded to the PV units. Finally, the procedure moves to the next time instant or terminates if the maximum number of time instants is reached.

III. Simulation Results

In this Section, simulation results on a 40-node unbalanced radial LV network are presented. Two different implementations of the APC and CAPC methods are investigated, namely the proposed phase-based and the positive-sequence-based approach of [15]. In the former, the single-phase active power injection is determined with respect to the corresponding phase-to-neutral PCC voltage, while in the latter, the positive-sequence voltage is used. In the next subsections, the system under study and the numerical results are presented.

A. System Under Study

The examined network is depicted in Fig. 3 and consists of 40 nodes. The network data concerning the rated power of all PV units and loads, as well as the line lengths are presented in Fig. 4. The lines are numbered according to the number of the corresponding ending node, e.g. line 38 is the line between nodes 37 and 38. In this network, single-phase as well as three-phase PV units and loads are considered. The power factor of all loads is assumed equal to 0.95 lagging, without loss of generality. The line impedance is 0.6538+*i*0.0769 Ω/km and 0.9393+*i*0.0909 Ω/km for the main (node 3 to node 28) and the remaining branches of the network, respectively.

Furthermore, at each network node, the neutral is grounded with an impedance of 2+*i*1 Ω. The 20/0.4 kV transformer has

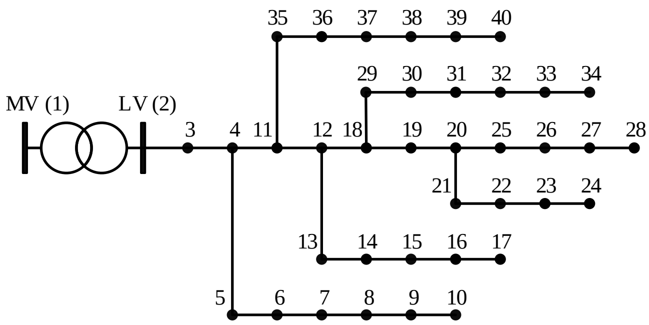

Fig. 3. Single line diagram of the examined network.

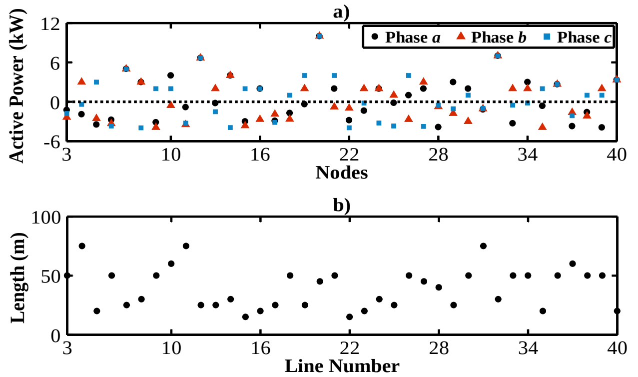

Fig. 4. Network data. (a) Rated active power of PV units and loads, and (b) lines length.

a nominal power of 250 kVA, short circuit voltage of 4%, while the full-load and no-load losses are 3300 W and 330 W, respectively. The voltage at the MV busbar of the transformer is deliberately set equal to 1.05 p.u. to ensure a sufficient voltage rise for the demonstration of droop control. However, this can also be a realistic case, since many DSOs manually change the tap of the MV/LV transformer to achieve a higher voltage at the LV busbar, avoiding undervoltages during high loading conditions.

B. Numerical Results

A single time instant is assumed, at which all PV units and loads initially operate at their rated power. The simulations are performed using the tool developed in [17]. The single-phase active power injections of all PV units for the different implementations of the APC and CAPC methods are presented in Figs. 5-7. Furthermore, the voltage profiles of the network are depicted in Figs. 8 and 9, while the corresponding zero- and negative-sequence voltage unbalance factors, as determined in [16], are shown in Figs. 10 and 11, respectively.

According to the simulation results, it is observed that both approaches of the APC method result in a non-uniform active power curtailment among the PV units connected to the same phase. Moreover, the positive-sequence implementation of the APC method (APC-POS) cannot effectively mitigate overvoltages. The reason lies in the fact that the positive-sequence implementation ignores the network asymmetries and thus it cannot effectively handle phase-to-neutral voltages. This can be verified in Fig. 8, where the voltage magnitude of phase *c* exceeds the maximum permissible voltage of 1.1 p.u. at several nodes.

The situation is improved when the phase-based implementation of the APC method (APC-PHA) is employed. According to Fig. 9, overvoltages are fully mitigated at all nodes. This happens since each phase is individually controlled, taking indirectly into account the network asymmetries. Furthermore, the APC-PHA control scheme results in reduced network asymmetries, since the corresponding voltage unbalance factors depicted in Fig. 10 and Fig. 11 are decreased for most network nodes. Therefore, the APC-PHA method presents an improved performance over the APC-POS control scheme, since overvoltages are fully mitigated and network asymmetries are further reduced.

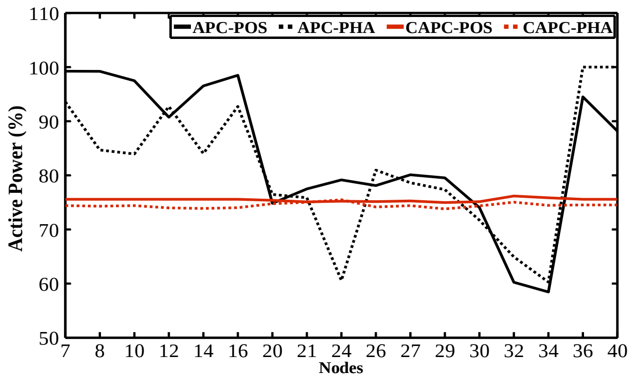

Fig. 5. Active power injection of the PV units connected to phase *a*.

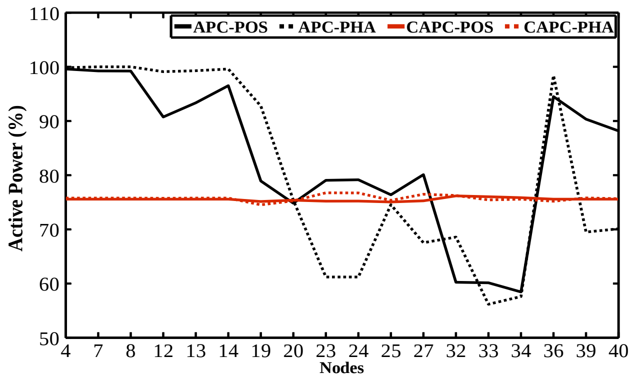

Fig. 6. Active power injection of the PV units connected to phase *b*.

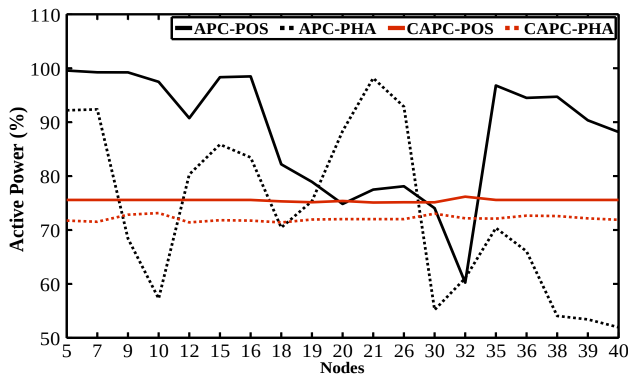

Fig. 7. Active power injection of the PV units connected to phase *c*.

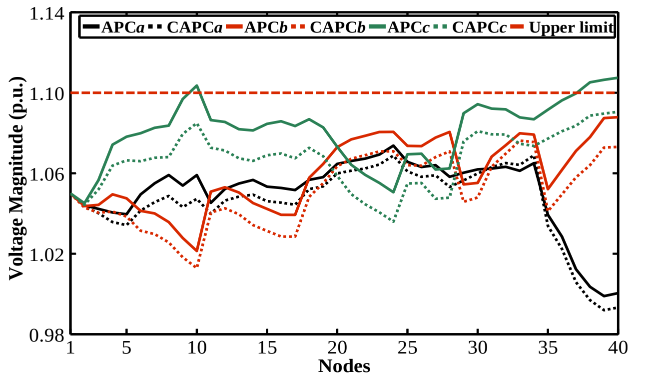

Fig. 8. Voltage profile of the network considering the positive-sequence implementation.

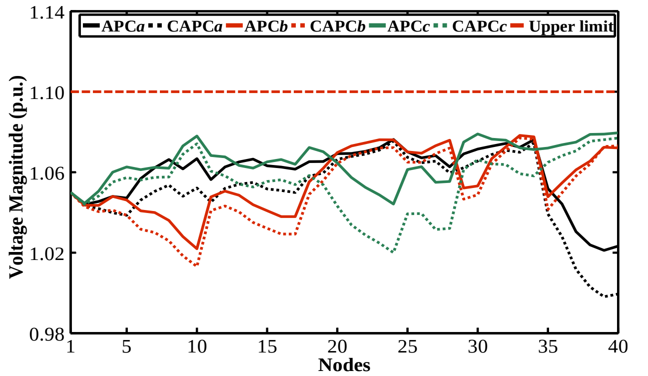

Fig. 9. Voltage profile of the network considering the phase-based implementation.

The common drawback of both implementations of the APC method is the non-uniform active power curtailment among the PV units of the same phase. Thus, the introduction of the CAPC method attempts to overcome this issue. According to Figs. 5-7, a uniform active power curtailment is achieved for both phase-based (CAPC-PHA) and positive-sequence-based (CAPC-POS) implementations of the CAPC method.

Nevertheless, the CAPC-POS control scheme assumes a balanced network by employing the positive-sequence voltages. Therefore, it cannot handle voltage asymmetries, presenting the same active power curtailment in each phase with the risk of possible voltage violations. On the other hand, the CAPC-PHA method redistributes the curtailed power based on the phase-to-neutral voltages. The voltage unbalance factors of the CAPC-PHA control scheme are reduced compared to the CAPC-POS implementation. Moreover, the CAPC methods result in almost similar voltage profiles to the APC methods, as shown in Figs. 8 and 9.

Tables I and II contain the overall active power injection and the corresponding network losses for all examined cases. The APC-POS and the CAPC-POS control schemes present higher power injections than the APC-PHA and the CAPC-PHA methods, respectively. However, this is case-dependent and cannot be considered as a general conclusion, while in all cases overvoltages are effectively tackled in the phase-based implementation, which is not guaranteed by the positive-

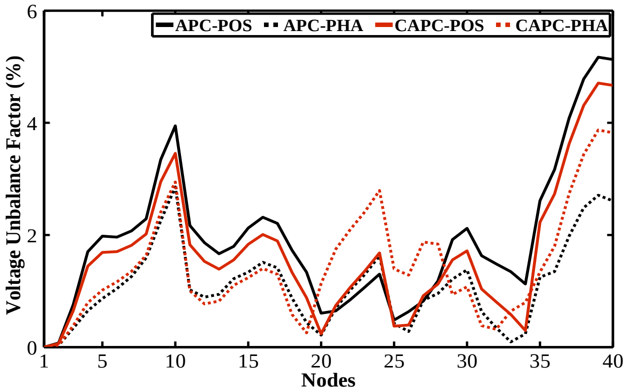

Fig. 10. Profile of the zero-sequence voltage unbalance factor.

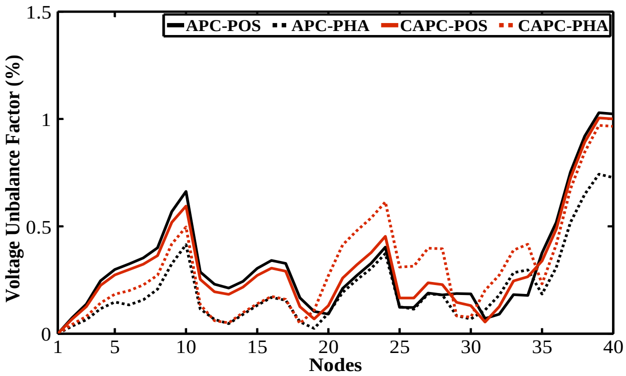

Fig. 11. Profile of the negative-sequence voltage unbalance factor.

TABLE I
OVERALL ACTIVE POWER INJECTION

	APC-POS	APC-PHA	CAPC-POS	CAPC-PHA
Active Power (kW)	157.726	152.085	142.772	139.975
Diff (%)		-3.58	-9.48	-11.25

TABLE II
ACTIVE POWER LOSSES

	APC-POS	APC-PHA	CAPC-POS	CAPC-PHA
Losses (kW)	3.283	2.867	2.949	2.852
Diff (%)		-12.67	-10.16	-13.14

sequence implementation. Additionally, the CAPC method results in less active power injections compared to the APC methods, but in a uniform and fairer way. Similar conclusions can be drawn for the network losses which are strongly related with the overall active power injection, since a reverse power flow occurs.

IV. CONCLUSIONS

In this paper, a coordinated phase-based voltage regulation algorithm is proposed, aiming to achieve a uniform active power curtailment among the PV units connected to the same phase. The proposed method is based on the exploitation of the sensitivity matrix in asymmetrical networks in order to redistribute the active power curtailment among the PV units of the same phase.

Simulations results on a 40-node highly unbalanced network reveal the superior performance of the proposed method over other conventional control schemes in terms of overvoltage mitigation, reduction of network asymmetries reduction, and uniform curtailment of active power.

The proposed methodology can be used as an efficient tool to tackle overvoltages in heavily unbalanced LV distribution grids with distributed single phase PV units.

REFERENCES

[1] R. A. R. Walling, R. Saint, R. C. Dugan, J. Burke, and L. A. Kojovic, "Summary of distributed resources impact on power delivery system," *IEEE Trans. Power Del.*, vol. 23, no. 3, pp. 1636–1644, Jul. 2008.

[2] C. L. Masters, "Voltage rise: The big issue when connecting embedded generation to long 11 kV overhead lines," *Power Eng. J.*, vol. 16, pp. 5–12, 2002.

[3] B. Zhang, A. Y. S. Lam, A. D. Domínguez-Garcia, and D. Tse, "An optimal and distributed method for voltage regulation in power distribution systems," *IEEE Trans. Power Syst.*, vol. 30, no. 4, pp. 1714–1726, Jul. 2015.

[4] R. Yan and T. K. Saha, "Voltage variation sensitivity analysis for unbalanced distribution networks due to photovoltaic power fluctuations," *IEEE Trans. Power Syst.*, vol. 27, no. 2, pp. 1078–1089, May 2012.

[5] A. Kulmala, S. Repo, and P. Järventausta, "Coordinated voltage control in distribution networks including several distributed energy resources," *IEEE Trans. Smart Grid*, vol. 5, no. 4, pp. 2010–2020, Jul. 2014.

[6] M. E. Elkhatib, R. El-Shatshat, M. M. A. Salama, "Novel coordinated voltage control for smart distribution networks with DG," *IEEE Trans. Smart Grid*, vol. 2, no. 4, pp. 598–605, Dec. 2011.

[7] G. C. Kryonidis, C. S. Demoulias, and G. K. Papagiannis, "A nearly decentralized voltage regulation algorithm for loss minimization in radial MV networks with high DG penetration," *IEEE Trans. Sustain. Energy*, early access.

[8] A. Samadi, R. Eriksson, L. Söder, B. G. Rawn, and J. C. Boemer, "Coordinated active power-dependent voltage regulation in distribution grids with PV systems," *IEEE Trans. Power Del.*, vol. 29, no. 3, pp. 1454–1464, June 2014.

[9] R. Kabiri, D. G. Holmes, B. P. McGrath, and L. G. Meegahapola, "LV grid voltage regulation using transformer electronic tap changing, with PV inverter reactive power injection," *IEEE J. Emerg. Sel. Topics Power Electron.*, vol. 3, no. 4, pp.1182–1192, Dec. 2015.

[10] N. R. Ullah, K. Bhattacharya, and T. Thiringer, "Wind farms as reactive power ancillary service providers-technical and economic issues," *IEEE Trans. Energy Convers.*, vol. 24, no. 3, pp. 661–672, Sep. 2009.

[11] K. De Brabandere, A. Woyte, R. Belmans, and J. Nijs, "Prevention of inverter voltage tripping in high density PV grids," in *19th EU-PVSEC*, Paris, France, 2004.

[12] R. Tonkoski and L. A. C. Lopes, "Voltage regulation in radial distribution feeders with high penetration of photovoltaic," in *IEEE Energy 2030*, Atlanta, U.S.A., 2008.

[13] T. L. Vandoorn, J. D. M. De Kooning, B. Meersman, and L. Vandevelde, "Voltage-based droop control of renewables to avoid on-off oscillations caused by overvoltages," *IEEE Trans. Power Del.*, vol. 28, no. 2, pp. 845–854, Apr. 2013.

[14] R. Tonkoski, L. A. C. Lopes, and T. H. M. El-Fouly, "Coordinated active power curtailment of grid connected PV inverters for overvoltage prevention," *IEEE Trans. Sustain. Energy*, vol. 2, no. 2, pp. 139–147, Apr. 2011.

[15] M. M. V. M. Ali *et al.*, "Fair power curtailment of distributed renewable energy sources to mitigate overvoltages in low-voltage networks," in *PowerTech, 2015 IEEE Eindhoven*, Jun. 2015, pp. 1–6.

[16] *Voltage characteristics of electricity supplied by public distribution networks*, Standard EN 50160:2010.

[17] G. C. Kryonidis *et al.*, "A simulation tool for extended distribution grids with controlled distributed generation," in *PowerTech, 2015 IEEE Eindhoven*, Jun. 2015, pp. 1–6 .